Discrete variable representation for highly excited states of hydrogen atoms in magnetic fields

Tasko P. Grozdanov,[1,2] Lidija Andric,[1] Corneliu Manescu,[1,*] and Ronald McCarroll[1]
[1]*Laboratoire de Dynamique des Ions, Atomes et Molécules (URA 774 du CNRS), Université Pierre et Marie Curie, 4 Place Jussieu T12-B75, 75252 Paris Cedex 05, France*
[2]*Institute of Physics, P.O. Box 57, 11001 Belgrade, Yugoslavia*
(Received 24 March 1997)

A discrete variable representation (DVR) appropriate for describing the highly excited states of hydrogen atoms in laboratory-strength magnetic fields is constructed by using a symmetry-adapted direct product of one-dimensional DVR's in parabolic coordinates related to generalized Gauss-Laguerre quadratures. The resulting sparse Hamiltonian matrix is used in an iterative (filter-diagonalization) procedure to obtain eigenvalues and eigenvectors in a given spectral domain. The method is applied to calculate eigenvalues and lifetimes of ''circular'' Rydberg states, as well as oscillator strengths for the excitation of highly excited states. [S1050-2947(97)07409-X]

PACS number(s): 32.60.+i

I. INTRODUCTION

The discrete variable representation (DVR) was introduced by Light, Hamilton, and Lill [1], and traditionally used (see, for example, Ref. [2] and references therein) mainly in chemical physics to describe a variety of phenomena such as rovibrational motions of the atoms in molecules, chemical reactions, and molecule-surface interactions. Loosely speaking, the DVR is an approximate discretized coordinate representation in which the potential-energy matrix is diagonal while the (multidimensional) kinetic-energy matrix is sparse. These properties are very desirable in applications of various iterative numerical methods which are suitable for treatments of multidimensional nonseparable systems represented by large Hamiltonian matrices.

Applications in atomic physics have mainly followed the Lagrange-mesh approach of Baye and Heenen [3]. This method provides a special class of DVR's with analytically calculable differential operators. Recent applications include the magnetized hydrogen atom [4,5], helium atom [6] and implementation of the R-matrix method [7]. The latter was inspired by previous work of Layton and Stade [8,9]. Among other DVR-based applications let us mention the time-dependent treatment of a hydrogen atom in a laser field [10] and our recent calculations of the photoionization cross sections of hydrogen atoms in very strong magnetic fields [11].

In the present paper, in Sec. II we construct a DVR which is appropriate for the treatment of highly excited states of hydrogen atoms in laboratory-strength magnetic fields. This DVR is equivalent to the Laguerre mesh introduced previously by Baye and Vincke [4]. These authors, however, used direct methods of diagonalization to solve (generalized) eigenvalue problems and restricted their calculations to low-lying states. Instead, in Sec. III, we briefly describe an iterative (filter-diagonalization [12]) method for extracting the eigenvalues and eigenvectors of large matrices in a given spectral domain. Results of our calculations are presented in Sec. IV, where the eigenvalues and lifetimes of highly excited ''circular'' states are compared with the results of other numerical methods and semiclassical estimates. In addition, oscillator strengths for the transitions from low-lying to highly excited states close to the ionization threshold are presented. Finally, some concluding remarks are given in Sec. V. Atomic units ($e=m_e=\hbar=1$) are used throughout the work except where explicitly stated.

II. DVR BASIS FUNCTIONS AND HAMILTONIAN MATRIX

Let us consider the motion of an electron in the Coulomb field of a proton (assumed to have an infinite mass) and in the presence of an external homogeneous magnetic field oriented along the z axis of a coordinate system centered at the proton. The exact integrals of motion (good quantum numbers) are the z component of the electronic angular momentum $L_z=m$ and the parity $\Pi_z=\pm 1$, corresponding to the reflection $z\rightarrow -z$. We can restrict our considerations to a subspace of states with fixed m and disregard the trivial dependence of the eigenfunctions on the azimuthal angle $[(2\pi)^{-1/2}\exp(im\varphi)]$, thereby reducing our problem to a two-dimensional one. Introducing scaled parabolic coordinates (u,v)

$$\frac{u}{\lambda}=(\rho^2+z^2)^{1/2}+z, \tag{2.1}$$

$$\frac{v}{\lambda}=(\rho^2+z^2)^{1/2}-z, \tag{2.2}$$

$$\rho\, d\rho\, dz=\frac{1}{4\lambda^3}(u+v)du\, dv, \tag{2.3}$$

we may write the Hamiltonian of our system in the forms

$$H=T+V(u,v)+\frac{\gamma}{2}m, \tag{2.4}$$

*Permanent address: Facultatea de Fizica, Universitatea Bucuresti, Romania.

$$T=\frac{2\lambda^2}{u+v}\left[-\frac{\partial}{\partial u}\,u\,\frac{\partial}{\partial u}-\frac{\partial}{\partial v}\,v\,\frac{\partial}{\partial v}+\frac{m^2}{4}\left(\frac{1}{u}+\frac{1}{v}\right)\right], \tag{2.5}$$

$$V(u,v)=-\frac{2\lambda}{u+v}+\frac{\gamma^2}{8\lambda^2}\,uv. \tag{2.6}$$

In the above equations (2.1)–(2.6), λ is an arbitrary scaling parameter and γ is magnetic field strength measured in units of $B_0=2.35\times10^5\ T$. The linear Zeeman shift $(\gamma/2)m$ in Eq. (2.4) is the only place where the sign of m enters, and potential (2.6) contains Coulomb and diamagnetic terms.

Following the general procedure [1,2], we construct the DVR basis using the orthonormal and complete (on the interval $0\leqslant u<+\infty$) set of functions

$$\Phi_n^{|m|}(u)=\left[\frac{n!}{(n+|m|)!}\right]^{1/2}L_n^{|m|}(u)u^{|m|/2}e^{-u/2},\quad n=0,1,2,\ldots, \tag{2.7}$$

where $L_n^{|m|}(u)$ are Generalized Laguerre polynomials. The one-dimensional DVR basis is then defined as follows:

$$y_\alpha^{|m|}(u)=w_\alpha^{1/2}\sum_{n=0}^{N-1}\Phi_n^{|m|}(u_\alpha)\Phi_n^{|m|}(u),\quad \alpha=1,2,\ldots,N, \tag{2.8}$$

where (u_α,w_α), $\alpha=1,2,\ldots,N$ [13] is the associated set of Nth-order generalized Gauss-Laguerre quadrature points and weights. Apart from being orthonormal, the basis functions (2.8) have the remarkable property

$$y_\alpha^{|m|}(u_\beta)=w_\alpha^{-1/2}\delta_{\alpha\beta}, \tag{2.9}$$

that is to say, they are zero at all quadrature points except one. In addition, the coordinate u is diagonal in the finite basis (2.8) with eigenvalues equal to the quadrature points

$$\int_0^{+\infty}y_\alpha^{|m|}(u)uy_\beta^{|m|}(u)du=u_\alpha\delta_{\alpha\beta}. \tag{2.10}$$

For treating our two-dimensional problem the next step is to form a direct-product DVR basis,

$$Y_{\alpha\beta}^{|m|}(u,v)=\frac{2\lambda^{3/2}}{(u_\alpha+v_\beta)^{1/2}}\,y_\alpha^{|m|}(u)y_\beta^{|m|}(v),\quad \alpha,\beta=1,2,\ldots,N. \tag{2.11}$$

The normalization factor follows from the form of the Jacobian (2.3) and the property (2.10).

However, as mentioned above, our Hamiltonian [Eqs. (2.4)–(2.6)] is invariant with respect to a reflection in the $z=0$ plane, which corresponds to an interchange $u\leftrightarrow v$ of parabolic coordinates. The basis functions (2.11) transform according to: $Y_{\alpha\beta}^{|m|}(v,u)=Y_{\beta\alpha}^{|m|}(u,v)$. Therefore, as our final basis we take either $N_{\rm DVR}=1/2N(N+1)$ symmetric or $N_{\rm DVR}=1/2N(N-1)$ antisymmetric combinations of the direct-product basis functions (2.11):

$$Y_{\alpha\beta}^{|m|\pm}(u,v)=\frac{Y_{\alpha\beta}^{|m|}(u,v)\pm Y_{\beta\alpha}^{|m|}(u,v)}{[2(1+\delta_{\alpha\beta})]^{1/2}},\qquad \alpha\leqslant\beta,\quad \alpha,\beta=1,2,\ldots,N. \tag{2.12}$$

All matrix elements are calculated by using the basic approximation of all DVR's [1,2], that is, the substitution of the exact integration by quadrature formulas. In our case, this corresponds to

$$\int_0^{+\infty}\int_0^{+\infty}f(u,v)du\,dv\approx\sum_{\alpha=1}^{N}w_\alpha\sum_{\beta=1}^{N}w_\beta f(u_\alpha,v_\beta). \tag{2.13}$$

Using this rule and property (2.9) it is easy to show that any function of coordinates is diagonal in DVR's. In particular, the matrix elements of the potential energy (2.6) are given by:

$$V_{\alpha\beta,\alpha'\beta'}=V(u_\alpha,v_\beta)\delta_{\alpha\alpha'}\delta_{\beta\beta'}. \tag{2.14}$$

Matrix elements of the kinetic energy operator (2.5) can be calculated by using the differential equation, satisfied by the $\Phi_n^{|m|}(u)$ functions:

$$\left(-\frac{\partial}{\partial u}\,u\,\frac{\partial}{\partial u}-\frac{m^2}{4u}+\frac{u}{4}\right)\Phi_n^{|m|}(u)=\left(n+\frac{|m|+1}{2}\right)\Phi_n^{|m|}(u). \tag{2.15}$$

In the symmetric and antisymmetric subspaces we find ($\alpha\leqslant\beta$, $\alpha'\leqslant\beta'$)

$$T^{\pm}_{\alpha\beta,\alpha'\beta'}=\frac{T_{\alpha\beta,\alpha'\beta}\pm T_{\alpha\beta,\beta'\alpha'}}{(1+\delta_{\alpha\beta})^{1/2}(1+\delta_{\alpha'\beta'})^{1/2}}, \tag{2.16}$$

with

$$T_{\alpha\beta,\alpha'\beta'}=\frac{2\lambda^2(t^u_{\alpha\alpha'}\delta_{\beta\beta'}+\delta_{\alpha\alpha'}t^v_{\beta\beta'})}{(u_\alpha+v_\beta)(u_{\alpha'}+v_{\beta'})}, \tag{2.17}$$

where, for example

$$t^u_{\alpha\alpha'}=w_\alpha^{1/2}w_{\alpha'}^{1/2}\sum_{n=0}^{N-1}\Phi_n^{|m|}(u_\alpha)\left(n+\frac{|m|+1}{2}\right)\Phi_n^{|m|}(u_{\alpha'})-\frac{u_\alpha}{4}\,\delta_{\alpha\alpha'}. \tag{2.18}$$

The sparse structure of the kinetic-energy matrix is obvious from Eq. (2.17), and actually only the ''one-dimensional'' matrix (2.18) needs to be stored in computer memory.

Finally, let us note that any wave function $\chi(u,v)$ (with well defined parity Π_z) is represented in our DVR by a vector with components ($\alpha\leqslant\beta$):

$$\chi_{\alpha\beta}=\langle Y_{\alpha\beta}^{|m|\pm}(u,v)|\chi(u,v)\rangle=\left[\frac{(u_\alpha+v_\beta)w_\alpha w_\beta}{2\lambda^3(1+\delta_{\alpha\beta})}\right]^{1/2}\chi(u_\alpha,u_\beta). \tag{2.19}$$

III. FILTER-DIAGONALIZATION METHOD

The basic idea of the method is due to Neuhauser [12]. The eigenvalues (and eigenvectors) of a given Hamiltonian H in a desired ''energy window'' $[E_{\min}, E_{\max}]$ are obtained by diagonalizing the Hamiltonian matrix in a small basis set of optimally adapted ''window'' functions $\{\psi_j\}$, $j=1,2,\ldots,N_{\rm win}$. Such a basis can be generated by acting with a suitable filtering operator $f(E-H)$ onto a generic initial wave packet χ:

$$\psi_j = f(E_j - H)\chi, \quad j=1,2,\ldots,N_{\rm win}, \tag{3.1}$$

where $E_{\min}<E_1<\cdots<E_j<\cdots<E_{N_{\rm win}}<E_{\max}$ and $f(x)$ is a function which is peaked at $x=0$ and decays rapidly for large $|x|$. Expanding the initial wave packet in the form $\chi = \Sigma_\alpha c_\alpha \phi_\alpha$ where $H\phi_\alpha = \epsilon_\alpha \phi_\alpha$, it is seen that each of the functions ψ_j is mainly composed of the eigenfunctions of H corresponding to eigenvalues close to E_j:

$$\psi_j = \sum_\alpha f(E_j - \epsilon_\alpha) c_\alpha \phi_\alpha . \tag{3.2}$$

It is the above mentioned form of the filtering function which suppresses the contribution in Eq. (3.2) from eigenstates ϕ_α with eigenvalues ϵ_α which are far away from E_j.

Originally [12], a Gaussian filter with adaptive width was used: $f(E-H)\sim\exp[-((E-H)/\sigma)^2]$. For the realization of the operator (matrix) action in Eq. (3.1) usually a polynomial expansion of $f(E-H)$ is used. In the present work we adopt an alternative filtering function [14], namely, the finite-width δ-function filter $f(E-H)=\delta_M(E-H)$. This function can be defined directly through its expansion in terms of Chebyshev polynomials $T_n(x)$:

$$\delta_M(E-H) = -\frac{2}{\Delta H \pi \sin\varphi(E)} \times \left[\frac{1}{2} + \sum_{n=1}^{M} \cos n\varphi(E)\, T_n(H_{\rm norm})\right], \tag{3.3}$$

with

$$T_0(H_{\rm norm}) = I, T_1(H_{\rm norm}) = H_{\rm norm}, \quad T_{n+1}(H_{\rm norm}) = 2H_{\rm norm}T_n(H_{\rm norm}) - T_{n-1}(H_{\rm norm}). \tag{3.4}$$

In the above, I is the unit matrix, and $H_{\rm norm}$ is the shifted and normalized Hamiltonian matrix:

$$H_{\rm norm} = \frac{H - \overline{H}I}{\delta H}, \tag{3.5}$$

where $\overline{H} = \frac{1}{2}(H_{\max}+H_{\min})$, $\Delta H = \frac{1}{2}(H_{\max}-H_{\min})$, and $H_{\max}$ and $H_{\min}$, respectively, are the upper and lower estimates of the maximum and minimum eigenvalues of the Hamiltonian matrix H. Thus, the spectrum of $H_{\rm norm}$ is confined to the segment $[-1,1]$. The dependence on E in Eq. (3.3) is contained in the phase

$$\varphi(E) = \arccos\left(\frac{E-\overline{H}}{\Delta H}\right). \tag{3.6}$$

The function $\delta_M(x)$ is peaked at $x=0$, and has a decaying oscillatory behavior at large $|x|$, fulfilling the above mentioned filtering property. As $M\to+\infty$, the expansion (3.3) tends toward the spectral density operator $\delta(E-H) = -(1/\pi)\mathrm{Im}G^+(E)$, and can be obtained from the Chebyshev-polynomial expansion of the Green's operator $G^+(E)=(E-H+i0)^{-1}$ [15].

Now combining Eqs. (3.1) and (3.3) [and neglecting the unimportant normalization factor in Eq. (3.3)], for the window-basis functions we obtain:

$$\psi_j = \tfrac{1}{2}\xi_0 + \sum_{n=1}^{M} \cos n\varphi(E_j)\,\xi_n , \tag{3.7}$$

where

$$\xi_0 = \chi, \quad \xi_1 = H_{\rm norm}\chi, \quad \xi_{n+1} = 2H_{\rm norm}\xi_n - \xi_{n-1} . \tag{3.8}$$

It is important to note that the E_j dependence in Eq. (3.7) is factored, so that a single iteration of Eq. (3.8) is sufficient to generate all basis functions ψ_j, $j=1,2,\ldots,N_{\rm win}$. After that, the basis set (3.7) can be Schmidt orthogonalized, and any linear dependence eliminated. The diagonalization of a Hamiltonian matrix in this small basis can than be performed by any of the standard methods. The quality of the obtained eigenvalues ϵ_α and eigenvectors ϕ_α can be checked by calculating the following estimate of the absolute error:

$$e_\alpha = \|(H-\epsilon_\alpha)\phi_\alpha\|. \tag{3.9}$$

The number of window-basis functions $N_{\rm win}$ should be, of course, larger than the number of eigenvalues in a given window. As a result of diagonalization in the small widow basis, the eigenvalues located outside the given window $[E_{\min},E_{\max}]$ will also appear, but with the errors (3.9) of orders of magnitude larger. The maximum number of window functions is limited by the available core memory of a computer. Wide spectral ranges of a very large matrices can be covered by a series of overlapping windows.

The main CPU time-consuming operation in the filter-diagonalization method is the matrix-vector multiplication in recursion (3.8). However, due to the sparseness of the Hamiltonian matrix in a DVR this is actually an $N_{\rm DVR}\ln N_{\rm DVR}$ process rather than a $N_{\rm DVR}^2$ process, and a very efficient coding of this operation is possible (see, for example, Ref. [2]).

Previous numerical experience [14,16] suggests that the number of terms M necessary in Eq. (3.7) in order to obtain well-converged eigenstates is given by the following empirical estimate

$$M \sim 2\Delta H \rho, \tag{3.10}$$

where $2\Delta H$ is the spectral range of the Hamiltonian matrix and ρ is the local spectral density.

IV. APPLICATIONS

The DVR Hamiltonian of Sec. II and the filter-diagonalization method explained in Sec. III are applied here for calculations of eigenvalues and radiative transition probabilities of highly excited states of hydrogen atoms in

TABLE I. Comparison of the calculated eigenenergies E (in 10^{-4} a.u.) of circular states with semiclassical estimates E^{SC} as predicted by the theory of Germann [18], for different values of the magnetic-field strength. The energies of the circular states with $m>0$ are obtained by adding γm.

	$m=-35$		$m=-39$		$m=-40$	
γ	E	E^{SC}	E	E^{SC}	E	E^{SC}
0	−3.858 0247	−3.858 0247	−3.125 0000	−3.125 0000	−2.974 4200	−2.974 4200
2×10^{-7}	−3.892 9384	−3.892 9384	−3.163 8688	−3.163 8688	−3.014 2753	−3.014 2753
2×10^{-6}	−4.199 4132	−4.199 4132	−3.501 9361	−3.501 9360	−3.360 0181	−3.360 0180
3×10^{-6}	−4.363 7037	−4.363 7035	−3.680 7594	−3.680 7589	−3.542 2102	−3.542 2096
4×10^{-6}	−4.523 8103	−4.523 8096	−3.853 3844	−3.853 3829	−3.717 6224	−3.717 6207
6×10^{-6}	−4.831 8667	−4.831 8636	−4.181 0541	−4.181 0480	−4.049 3618	−4.049 3548
1×10^{-5}	−5.402 9624	−5.402 9450	−4.774 4253	−4.774 3975	−4.646 5193	−4.646 4887
1.4×10^{-5}	−5.921 7731	−5.921 7283	−5.300 7072	−5.300 6443	−5.173 1889	−5.173 1220
2×10^{-5}	−6.621 0925	−6.620 9878	−5.996 6114	−5.996 4831	−5.866 7507	−5.866 6181
3×10^{-5}	−7.631 0714	−7.630 8425	−6.984 4737	−6.984 2229	−6.847 9021	−6.847 6481
4×10^{-5}	−8.504 4753	−8.504 1096	−7.829 0090	−7.828 6279	−7.684 8587	−7.684 4760
6×10^{-5}	−9.986 3690	−9.985 7123	−9.250 3774	−9.249 7212	−9.091 3259	−9.090 6717
1×10^{-4}	−12.335 253	−12.333 972	−11.487 385	−11.486 139	−11.301 886	−11.300 648
1.4×10^{-4}	−14.222 650	−14.220 703	−13.276 965	−13.275 087	−13.068 763	−13.066 902
2×10^{-4}	−16.561 837	−16.558 835	−15.488 608	−15.485 732	−15.251 052	−15.248 208

laboratory-strength magnetic fields. The first application deals with ''circular'' Rydberg states with a large angular momentum (see, for example [17,18] and references therein) while the second one concerns calculations of oscillator strengths for transitions from low-lying states to highly excited states close to the continuum border.

A. Eigenvalues and lifetimes of circular Rydberg states

''Circular'' Rydberg states in magnetic fields are the ''ground'' states of various m manifolds, with $|m|\gg1$ and well-defined parity $\Pi_z=+1$. The name comes from the fact that the electron is localized in the vicinity of a circular orbit perpendicular to the field direction [18]. Being located at the edge of the spectrum of the manifold, where the local spectral density is small, these eigenstates are relatively easy to obtain with the filter-diagonalization method.

Results of our calculations of the energies of circular states with $m=-35$, -39, and -40 in the range of magnetic-field strengths $\gamma=0-2\times10^{-4}(B=0-47$ T) are shown in Table I. They were obtained by using $N=40$ one-dimensional DVR basis functions, that, is the total of $N_{\rm DVR}=\frac{1}{2}N(N+1)=820$ two-dimensional basis functions (or DVR grid points) with the value of the scaling parameter $\lambda=0.03$. $N_{\rm win}=50-100$ window functions were used and only $M=300$ iterations in Eqs. (3.7) and (3.8) were necessary to obtain errors $e_\alpha<10^{-9}$ a.u. for circular and nearby states. The initial, generic wave packet χ was taken either randomly or uniformly over the DVR grid with no difference in performance of the method.

Eigenvalues for $m=-35$ were previously calculated in Ref. [17] by diagonalization of a banded Hamiltonian matrix constructed in the basis of 70 radial Sturmians and 70 spherical harmonics. We found the agreement with these results to all eight significant figures shown in Table I.

For further comparisons, also shown in Table I are the semiclassical results which we calculated using the formulas recently derived by Germann [18]. This approach is actually an extension of the previous work of Ref. [19]. It is based on an expansion in terms of the small parameter $\delta=(|m|+1)^{-1}$. The crucial quantity is the scaled radius $\tilde{\rho}_m$ of the circular orbit in $z=0$ plane around which the electron is localized. It is defined as the location of the minimum of an effective potential

$$V_{\rm eff}(\tilde{\rho})=\frac{1}{2\tilde{\rho}^2}-\frac{1}{\tilde{\rho}}+\frac{\tilde{\gamma}^2\tilde{\rho}^2}{8}, \tag{4.1}$$

where $\tilde{\rho}=\delta^2\rho$ and $\tilde{\gamma}=\delta^{-3}\gamma$. The energy of a circular state is then given by

$$\epsilon_m^{sc}=\frac{m\gamma}{2}+\delta^2V_{\rm eff}(\tilde{\rho}_m)+\tfrac{1}{2}\delta^3\left(\omega_1+\omega_2-\frac{1}{\tilde{\rho}_m^2}\right), \tag{4.2}$$

where the frequencies

$$\omega_1^2=\frac{3}{\tilde{\rho}_m^4}-\frac{2}{\tilde{\rho}_m^3}+\frac{\tilde{\gamma}^2}{4}, \quad \omega_2^2=\frac{1}{\tilde{\rho}_m^3} \tag{4.3}$$

are related to oscillations of the electron perpendicular to the circular orbit. As can be seen from Table I, the simple semiclassical expression (4.2) reproduces 4–7 significant figures of the exact results. This excellent agreement confirms the highly ''semiclassical nature'' of circular states. In accord with the findings of Ref. [19], the semiclassical eigenvalues become less accurate at larger magnetic-field strengths.

The only allowed radiative electric-dipole transition from a circular state is to the neighboring circular state with one less quantum of angular momentum: $m\to m'$, $|m'|=|m|-1$. The lifetime τ_m of a circular state is therefore given by

$$\tau_m^{-1}=\frac{4}{3c^3}(\epsilon_m-\epsilon_{m'})^3|d_{m',m}|^2, \tag{4.4}$$

TABLE II. Comparison of the calculated lifetimes τ (in milliseconds) of circular states with the results of Ref. [17], τ^W, and with semiclassical estimates τ^{SC} as predicted by the theory of Germann [18], for different values of the magnetic field strength.

	$m=+35$			$m=-40$		$m=+40$	
γ	τ	τ^W	τ^{SC}	τ	τ^{SC}	τ	τ^{SC}
0	5.489	5.498	5.584	10.55	10.71	10.55	10.71
2×10^{-7}	5.416	5.425	5.509	10.77	10.92	10.34	10.50
2×10^{-6}	4.776	4.756	4.857	12.71	12.89	8.558	8.680
3×10^{-6}	4.441	4.447	4.514	13.79	13.98	7.662	7.767
4×10^{-6}	4.122	4.128	4.189	14.86	15.05	6.847	6.936
6×10^{-6}	3.543	3.547	3.597	16.85	17.04	5.465	5.528
1×10^{-5}	2.617	2.620	2.650	20.14	20.31	3.561	3.590
1.4×10^{-5}	1.960	1.962	1.980	22.49	22.62	2.436	2.450
2×10^{-5}	1.325	1.327	1.335	24.69	24.79	1.507	1.512
3×10^{-5}	0.770	0.771	0.774	26.39	26.44	0.808	0.809
4×10^{-5}	0.498	0.498	0.499	26.91	26.94	0.500	0.501
6×10^{-5}	0.250	0.255	0.255	26.69	26.69	0.245	0.245
1×10^{-4}	0.103	0.103	0.103	25.10	25.08	0.0962	0.0961
1.4×10^{-4}	0.0556	0.0557	0.0556	23.51	23.48	0.0510	0.0509
2×10^{-4}	0.0285	0.0285	0.0284	21.56	21.53	0.0258	0.0258

with the dipole matrix element ($m'=m\pm1$):

$$d_{m',m}=\mp2^{-1/2}\langle\psi_{m'}(\rho,z,\varphi)|\rho e^{\pm i\varphi}|\psi_m(\rho,z,\varphi)\rangle. \tag{4.5}$$

As the output of our filter-diagonalization calculations we obtain the eigenvalues ϵ_m and $\epsilon_{m'}$ as well as the DVR components $\phi^{|m|}_{\alpha,\beta}$ and $\phi^{|m'|}_{\alpha',\beta'}$ of the eigenvectors. Since DVR's are $|m|$-dependent (see Sec. II), in order to calculate matrix elements (4.5) it is necessary to transform to a single DVR (say to the one related to $|m|$). This transformation can be derived from general expression (2.19) and is given by

$$\phi^{|m'|}_{\alpha,\beta}=\left[\frac{(u_\alpha+v_\beta)w_\alpha w_\beta}{2\lambda^3(1+\delta_{\alpha\beta})}\right]^{1/2}\sum_{\alpha'\leqslant\beta'}\phi^{|m'|}_{\alpha',\beta'}Y^{|m'|+}_{\alpha',\beta'}(u_\alpha,v_\beta). \tag{4.6}$$

Now, the dipole matrix elements (4.5) can be simply calculated as

$$d_{m',m}=\mp2^{-1/2}\sum_{\alpha\leqslant\beta}\phi^{|m'|}_{\alpha,\beta}\frac{(u_\alpha v_\beta)^{1/2}}{\lambda}\phi^{|m|}_{\alpha,\beta}. \tag{4.7}$$

Results of our calculations of the lifetimes are shown in Table II, for circular states with $m=+35$ and ±40 and the range of magnetic-field strengths $\gamma=0-2\times10^{-4}$($B=0-47$ T). The comparison with the calculations of Ref. [17] is also presented. We see that, contrary to the case of the eigenvalues, there appear to be some small differences. The origin of the discrepancy is unknown, but one can see that it persists even in the limit $B=0$. In this limit, however, one can analytically calculate the lifetime of a circular state (that is, of a hydrogenic state with spherical quantum numbers $\{n=|m|+1,\ l=|m|,\ m\}$):

$$(\tau^0_m)^{-1}=\frac{4}{3c^3}\left(\frac{1}{2|m|^2}-\frac{1}{2(|m|+1)^2}\right)^3|d^0_{m',m}|^2, \tag{4.8}$$

where

$$|d^0_{m',m}|=\frac{2^{2|m|+(5/2)}(|m|+1)^{|m|+2}|m|^{|m|+3}}{(2|m|+1)^{2|m|+3}}. \tag{4.9}$$

The above exact formula gives lifetimes which coincide with the results of our calculations.

Also shown for comparison in Table II are the predictions of the semiclassical approach of Germann [18]. The dipole matrix elements are calculated according to the formula

$$d^0_{m',m}=\mp\frac{(\omega_1\omega_2\omega_1'\omega_2')^{1/4}(\delta\delta')^{3/2}}{2b(2\pi a)^{1/2}}\exp\left(-\frac{\omega_1\tilde{\rho}_m^2}{2\delta}-\frac{\omega_1'\tilde{\rho}_m'^2}{2\delta'}\right)\times\left[1+c\left(\frac{\pi}{b}\right)^{1/2}\exp\left(\frac{c^2}{4b}\right)\right], \tag{4.10}$$

where $a=\frac{1}{2}(\omega_2\delta^3+\omega_2'\delta'^3)$, $b=\frac{1}{2}(\omega_1\delta^3+\omega_1'\delta'^3)$, and $c=\omega_1\tilde{\rho}_m\delta+\omega_1'\tilde{\rho}_m'\delta'$. [In Eq. (15) of Ref. [18] the factor $(\delta\delta')^{3/2}$ is missing]. As can be seen from Table II, the semiclassical lifetimes agree very well with the quantum-mechanical values over a wide range of magnetic-field strengths. This means that the approximate wave functions of Germann [18], given as simple products of Gaussians centered at $z=0$ and $\tilde{\rho}=\tilde{\rho}_m$, are very good approximations to the exact eigenfunctions.

B. Photoexcitation of highly excited states

In order to test our method further, we applied it to calculations of the eigenvalues and eigenvectors in the regions of high local spectral density. To our knowledge, the tabulated eigenvalues of the converged numerical calculations for highly excited states exist only in the work of Clark and Taylor [20] based on the expansions in terms of radial Sturmians and spherical harmonics. The tabulated energies, however, correspond to the so called l-mixing regime (where the principal quantum number n is approximately conserved)

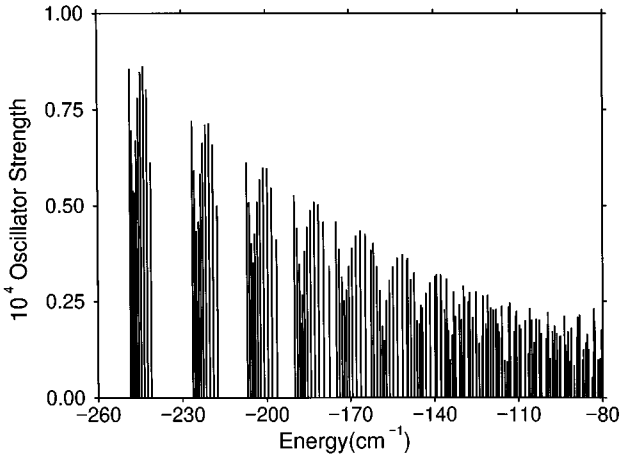

FIG. 1. The oscillator strengths for transitions from $3s$ state of hydrogen atom into $m=0$, odd-parity Rydberg states in a magnetic field of 6.1 T.

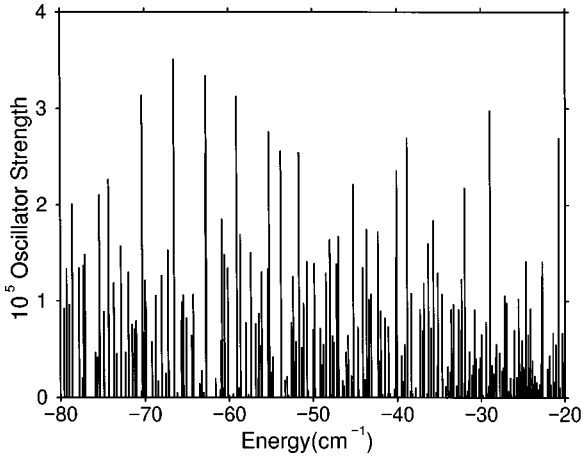

FIG. 2. The same as Fig. 1, but at energies closer to the ionization threshold.

and cover the cases of five manifolds with $n=23$, $m=0,1,2$, $\Pi_z=\pm 1$ at a field strength $B=4.7$ T. We have found it comparatively easy to reproduce with our method all seven significant figures of the eigenvalues listed in Ref. [20].

As a more challenging task we have chosen to reproduce the results of the R-matrix calculations of O'Mahony [21]. We therefore study the photoexcitation, from an initial $3s$ state of a hydrogen atom in a field of $B=6.1$ T by photons linearly polarized along the field direction. The final states are highly excited odd-parity ($\Pi_z=-1$) states of the $m=0$ manifold. The quantities calculated are oscillator strengths

$$f_{3s,f}=2(\epsilon_f-\epsilon_{3s})z_{3s,f}, \tag{4.11}$$

where

$$z_{3s,f}=\langle \psi_{3s}(\rho,z,\varphi)|z|\psi_f(\rho,z,\varphi)\rangle. \tag{4.12}$$

As a result of our DVR-filter-diagonalization method, we have eigenvalues ϵ_f and DVR components $\phi^f_{\alpha\beta}$ of the final-state eigenvectors. The dipole matrix element (4.12) is than given by

$$z_{3s,f}=\sum_{\alpha<\beta}\phi^{3s}_{\alpha\beta}\,\frac{u_\alpha-v_\beta}{2\lambda}\,\phi^f_{\alpha\beta}, \tag{4.13}$$

where $\phi^{3s}_{\alpha\beta}$ are the DVR components of the hydrogenic $3s$ wave function which can be found from the general formula (2.19).

Results of our calculations for the range of final-state energies $[-260,-80]$ cm^{-1} are shown in Fig. 1, while those covering the range $[-80,-20]$ cm^{-1} are presented in Fig. 2. No visible difference can be found with the results of R-matrix calculations [21]. As can be seen from Fig. 1 at lower energies, n manifolds are well separated (l-mixing regime) and characterized by regular distributions of oscillator strengths which are repeated in each of the manifolds. At higher energies manifolds begin to overlap (n-mixing regime) and the regularity in the distribution of oscillator strengths disappears. At even higher energies, closer to the ionization threshold, as seen from Fig. 2, a completely irregular pattern appears. It is well known that this transformation of the spectrum closely follows the transition from regular to chaotic classical motion of the Rydberg electron (see, for example, Ref. [22]).

Results presented in Figs. 1 and 2 have been obtained by using six overlapping energy windows with $N_{\rm win}=200$ window-basis functions in each of them. The parameters of the DVR basis were in the ranges $N=40-100$ ($N_{\rm DVR}=780-4950$), $\lambda=0.05-0.02$, and the number of iterations $M=(2-10)\times 10^5$, corresponding, respectively, to lowest and highest energies considered. This has been enough to achieve convergence (with respect to variations of N and λ) to six significant figures of the eigenvalues and 2–3 figures of oscillator strengths, while the quoted number of iterations was needed to obtain absolute errors of the eigenvalues of the matrices $e_\alpha<10^{-7}$ cm^{-1}.

A very large number of iterations is related to the high local spectral density and is in accord with estimate (3.10). Although our results confirm the high numerical stability of the Chebyshev recursion relations (3.8) with respect to the roundoff errors, large numbers of iterations represent clearly limitation of the method (but see the discussion in Sec. V). The calculations in the uppermost windows took tens of CPU hours on an IBM 6000/370 workstation.

V. CONCLUDING REMARKS

In the present work, we have demonstrated that the proposed DVR can successfully be applied to treating bound-state problems of a highly excited hydrogen atom in laboratory-strength magnetic fields. Extensions to problems of the continuous spectrum, such as calculations of resonances or photoionization cross sections, are possible by the use of absorbing boundary conditions and corresponding polynomial expansions of Green's operator [11,14].

One of the main advantages of any DVR is the absence of the necessity to calculate multidimensional matrix elements numerically, because the potential energy matrix is diagonal and can be trivially obtained. In the case of a hydrogen atom perturbed by external magnetic and electric fields the traditional use of the Sturmian basis [20] results in (analytically calculable) banded Hamiltonian matrices. This is, however, a

consequence of the fact that the perturbing potentials are polynomials in electronic coordinates. On the other hand, the DVR introduced in Sec. II can be applied to any cylindrically symmetric potential (for example, core potential of a nonhydrogenic atom, as well as electric field parallel to the magnetic field can be added). The treatment of fully three-dimensional problems (without cylindrical symmetry), can easily be developed by including into the direct product an additional one-dimensional DVR corresponding to the azimuthal angle φ.

The sparseness of a Hamiltonian matrix in the DVR is very useful for efficient coding of the iterative methods which are inevitable when dealing with matrices of very large dimensions. In the present work we used the form of the filter-diagonalization method which becomes very CPU time consuming when dealing with a very high density of states. However, we note that recently [16], significant improvements of the method have been developed which speed up the recursive procedure and reduce the spectral range of the Hamiltonian, and thus make it more efficient. Of course, once the DVR of a Hamiltonian is constructed, one is not limited to this method. For example, the possible alternatives are the iterative methods based on the Lanczos algorithm [23].

ACKNOWLEDGMENTS

T.P.G. and C.M. are grateful for the hospitality shown by the Laboratoire de Dynamique des Ions, Atomes et Molécules, Université Pierre et Marie Curie where part of this work has been done. T.P.G. acknowledges support of this work by the Ministry of Science and Technology of the Republic of Serbia.

[1] J. C. Light, I. P. Hamilton, and J. V. Lill, J. Chem. Phys. **82**, 1400 (1985).
[2] G. C. Groenenboom and D. T. Colbert, J. Chem. Phys. **99**, 9681 (1993).
[3] D. Baye and P.-H. Heenen, J. Phys. A **19**, 2041 (1986).
[4] D. Baye and M. Vincke, J. Phys. B **24**, 3551 (1991).
[5] M. Vincke, L. Malegat, and D. Baye, J. Phys. B **26**, 811 (1993).
[6] L. Malegat and M. Vincke, J. Phys. B **27**, 645 (1994).
[7] L. Malegat, J. Phys. B **27**, L691 (1994).
[8] E. G. Layton, J. Phys. B **26**, 2501 (1993).
[9] E. G. Layton and E. Stade, J. Phys. B **26**, L489 (1993).
[10] J. T. Muckerman, R. V. Weaver, T. A. B. Kennedy, and T. Uzer, in *Numerical Grid Methods and their Applications to Schrödinger Equation*, edited by C. Cerjan (Kluwer, Dordrecht, 1993), p. 89.
[11] T. P. Grozdanov and R. McCarroll, J. Phys. B **29**, 3373 (1996).
[12] D. Neuhauser, J. Chem. Phys. **93**, 2611 (1990); **100**, 5076 (1994); M. R. Wall and D. Neuhauser, *ibid.* **102**, 8011 (1995).
[13] G. H. Golub and J. H. Welsch, Math. Comput. **24**, 221 (1968).
[14] V. A. Mandelshtam and H. S. Taylor, J. Chem. Phys. **102**, 7390 (1995); T. P. Grozdanov, V. A. Mandelshtam, and H. S. Taylor, *ibid.* **103**, 7990 (1995); V. A. Mandelshtam, T. P. Grozdanov, and H. S. Taylor, *ibid.* **103**, 10 074 (1995).
[15] B. Hartke, R. Kosloff, and S. Ruhman, Chem. Phys. Lett. **158**, 238 (1989); R. Kosloff, J. Phys. Chem. **92**, 2087 (1988); Y. Huang, W. Zhu, D. J. Kouri, and D. K. Hoffman, Chem. Phys. Lett. **206**, 96 (1993).
[16] V. A. Mandelshtam and H. S. Taylor, J. Chem. Soc. Faraday Trans. **93**, 847 (1997).
[17] G. Wunner, M. Kost, and H. Ruder, Phys. Rev. A **33**, 1444 (1986).
[18] T. C. Germann, J. Phys. B **28**, L531 (1995).
[19] C. M. Bender, L. D. Mlodinow, and N. Papanicolaou, Phys. Rev. A **25**, 1305 (1982).
[20] C. W. Clark and K. T. Taylor, J. Phys. B **15**, 1175 (1982).
[21] P. F. O'Mahony, Phys. Rev. Lett. **63**, 2653 (1989).
[22] H. Friedrich and D. Wintgen, Phys. Rep. **183**, 37 (1989).
[23] C. K. Cullum and R. A. Willoughby, *Lanczos Algorithms for Large Symmetric Eigenvalue Computations* (Birkhäuser, Boston, 1985).